ARTICLES

Structure and energetics of antiferroelectric $PbZrO_3$

David J. Singh
Complex Systems Theory Branch, Naval Research Laboratory, Washington, D.C. 20375
(Received 31 May 1995)

Structural instabilities and electronic properties of $PrZrO_3$ are investigated using local-density calculations. Substantial hybridization is found in the electronic band structure, both between O $2p$ and Zr $4d$ states and between O $2p$ and Pb s and p states. A very strong Γ point phonon instability is present for the cubic perovskite structure. Relaxation, allowing only zone-center distortions, yields a large energy lowering of 0.253 eV, with bond-length changes in excess of 0.5 Å. Two related R point instabilities are found, both of which involve changes in Pb-O distances. The more unstable of these involves a 12° rotation of the O octahedra, with an energy lowering of 0.20 eV per formula unit. Total-energy calculations were performed for 40 atom unit cells with orthorhombic $Pba2$ and $Pbam$ space groups as reported experimentally. Energies close to but still above the related Γ structure were obtained with experimentally determined atomic positions. However, after relaxation of the oxygen coordinates, the antiferroelectric structure is favored by 0.02 eV per formula unit. This ordering and the small ferroelectric-antiferroelectric energy difference is in accord with the $Pb(Zr,Ti)O_3$ phase diagram.

INTRODUCTION

Perovskite oxides, ABO_3, particularly with a transition-metal B atom, display a wide variety of interesting and complex structural instabilities and widely varying electronic properties. These include ferroelectric and antiferroelectric distortions, and electronic properties from metallic (and in related phases superconducting) to wide band-gap insulators. $PbZrO_3$ is of particular interest both as an end point of the technologically important $Pb(Zr,Ti)O_3$ (PZT) alloy system, and because of the rich temperature and composition dependent phase diagram near this end point.

The PZT phase diagram[1] consists of a paraelectric cubic phase at high temperatures. Above about 50% Ti, there is a single lower temperature tetragonal ferroelectric phase with a transition temperature ranging from about 350 °C at the 50% composition to near 500 °C for pure $PbTiO_3$. This transition has been investigated in detail by Cohen and co-workers,[2,3] using detailed first-principles calculations. They find a strong ferroelectric instability of approximately 0.1 eV per formula unit relative to the cubic perovskite structure, consistent with the experiment. Moreover, they obtain a very good description of the ground-state structure including even the correct tetragonal strain. The differences from $BaTiO_3$ which has only a very weak instability and a rhombohedral ground state are ascribed to the substantial Pb $6s$–O $2p$ hybridization. Both materials show significant hybridization between Ti $3d$ and O $2p$ states. This is a particularly interesting feature of transition-metal perovskites and has been identified as an important ingredient in causing ferroelectric instabilities.[2–4]

The phase diagram near $PbZrO_3$ is considerably richer. Below approximately 230 °C, $PbZrO_3$ occurs in a complex antiferroelectric orthorhombic (AFO) structure with eight formula units per cell.[5–10] A small tetragonal antiferroelectric region has also been reported at low doping near the high-temperature transition.[10] For Ti concentrations above 1%, the initial temperature-dependent transition from the cubic phase is to a rhombohedral ferroelectric phase, similar in structure to the low-temperature phases of $BaTiO_3$ and $KNbO_3$; this then transforms at lower temperature the AFO ground state. This ferroelectric phase has also been reported in a narrow temperature range for pure $PbZrO_3$. The transition to the AFO phase is strongly depressed with increasing Ti concentrations, disappearing at about 7% Ti; above this concentration, the low-temperature transition is instead to a more complex rhombohedral ferroelectric structure with rotated oxygen octahedra.

Although they are isoelectric elements, changes in the electronic structure are expected upon substituting Zr for Ti in the PZT system. In particular, the $4d$ transition metals have considerably more extended d orbitals than the $3d$ elements, leading to the expectation of greater covalency with O $2p$ states in the zirconate. The unit-cell volume difference of about 10% is relatively small, and in particular is approximately half of that expected based on the change in ionic radius for a cubic perovskite structure, again implying increased covalency in the zirconate. Here, first-principles methods, based on density-functional theory, are used to investigate the electronic properties, energetics and structure of $PbZrO_3$.

METHOD

The present calculations were performed, within the local-density approximation (LDA) using a local orbital extension[11] of the general potential linearized augmented plane-wave (LAPW) method,[12,13] as in previous investigations of $KNbO_3$ and $BaTiO_3$.[14,15] The exchange-correlation

parametrization was that of Hedin and Lundqvist.[16] Core states were calculated relativistically, while valence states were calculated semirelativistically. Spin-orbit interactions, which are of some importance in describing Pb and some Pb compounds, could be neglected because the Pb $6p$ derived bands in oxides occur well above the Fermi energy, and because of this their spin-orbit splittings do not contribute significantly to the energetics. Well converged basis sets[17] consisting of approximately 750 functions per formula unit were employed. This resulted in basis sets in excess of 6000 basis functions for the AFO structure. Brillouin-zone samplings were performed using the special points method. An $8\times8\times8$ mesh was used for the cubic perovskite structure and Γ point distortions, although it was found that a $6\times6\times6$ mesh yielded the same energetics to within 0.1 mRy. Meshes of at least this reciprocal space density (note that due to zone folding this corresponds to fewer k points for larger unit cells) were used for the final energy calculations in the other structures. The energy and force convergence was explicitly tested for the final AFO structure, by comparing energies calculated with 6 k points to those calculated with 2 k points. Structural relaxations were performed with calculations of the atomic forces, based on the method of Yu, Singh, and Krakauer.[18]

CUBIC PEROVSKITE STRUCTURE

Calculations of the total energy of cubic perovskite structure $PrZrO_3$ as a function of volume yielded a lattice parameter of 4.12 Å and a bulk modulus of 180 GPa. This lattice parameter is essentially the same as that obtained by King-Smith and Vanderbilt using an ultrasoft pseudopotential method.[19] The cell volume is only 1% smaller than the experimental volume at room temperature, although it should be noted that the experimental structure is distorted AFO. The zone-center (Γ point) phonons and the Γ and R point instabilities were calculated at this lattice parameter, while the AFO structure was calculated using the experimentally determined lattice parameters.

The band structure of cubic perovskite $PbZrO_3$ is shown in Fig. 1; the corresponding total and LAPW sphere projected electronic density of states (DOS) is shown in Fig. 2. The band structure shows a valence band region, consisting of a manifold of nine bands, nominally derived from the oxygen $2p$ states (a Pb $5s$ derived band is separated below and is the lowest band in the band-structure plot). The valence bands are separated by a 2.34 eV direct gap at X from the conduction band states. Although the band edge is of primarily Pb $6p$ character, the conduction bands have strong contributions from both the Pb $6p$ and Zr $4d$ states, as is evident from the projected DOS. Examination of the DOS reveals that there is also substantial O $2p$ character in the conduction bands. This is particularly striking in view of the relatively small 1.55 a.u. O sphere radius used in this study, which would tend to underweight O projections. Conversely, there are strong Zr $4d$ and Pb $5p$ contributions to the valence band DOS. These contributions, particularly the Zr $4d$ weight, are enhanced in the lower part of the valence bands relative to the upper part, indicating quite strong covalent bonding effects.

The lowest valence band has a minimum at the R point.

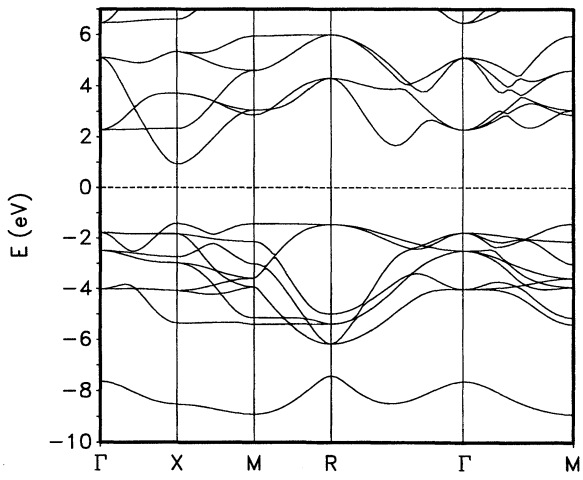

FIG. 1. Band structure of cubic perovskite $PbZrO_3$. The dashed horizontal line denotes the Fermi energy.

Unlike the band structures of $BaTiO_3$ and $KNbO_3$,[15] the lowest valence band at R is significantly lower (by 0.77 eV) than the lowest band at M. In $PbZrO_3$, the lowest band at R has significant Pb $6p$ character, which based on the weights in the spheres, is approximately equal to the Zr $4d$ character, while the lowest band at M has no Pb $6p$ character. This is indicative of bonding involving Pb $6p$ and O $2p$ states in addition to the Zr $4d$–O $2p$ interactions. This differs from $KNbO_3$ and $BaTiO_3$, where the A site cation is inactive, and explains qualitatively the difference from those compounds.

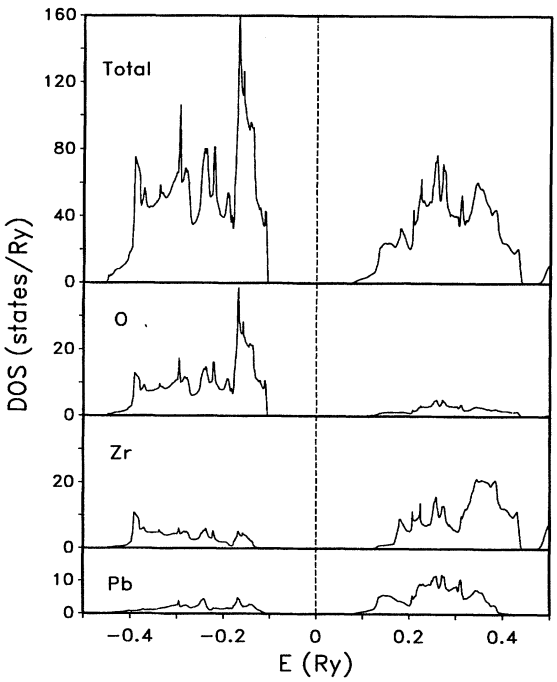

FIG. 2. Total and projected electronic DOS for cubic perovskite $PbZrO_3$. The projections are on a per atom basis and are the total DOS weighted by contributions from the LAPW sphere in question.

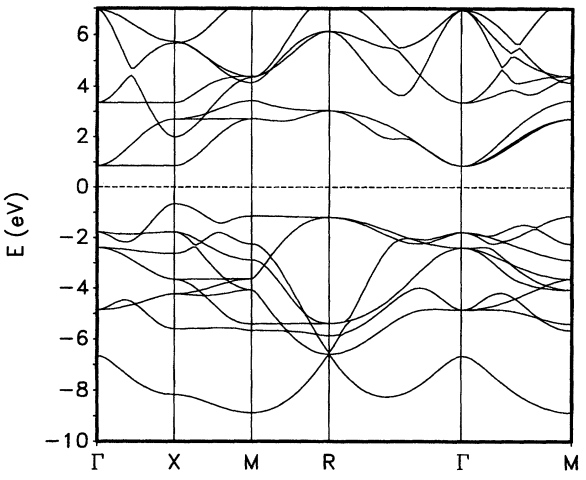

FIG. 3. Band structure of cubic perovskite $PbTiO_3$.

The band structure from parallel calculations on $PbTiO_3$ is shown in Fig. 3. It is essentially the same as that obtained by King-Smith and Vanderbilt,[19] and is qualitatively like that of $PbZrO_3$ (Fig. 1). The main differences between the two materials are as follows: (1) the valence bands are broader in the titanate with the main broadening occurring near the bottom of the bands so that the R point minimum is now deep enough to touch the Pb $6s$ derived bands, which are also broadened. This correlates with the reduced lattice parameter and Pb-O distance in the titanate, again illustrating the importance of Pb-O interactions in these materials; (2) the conduction bands are narrower in the titanate, with generally weaker band dispersions. This reflects reduced hybridization of transition-metal d and O p states in the titanate relative to the zirconate. Thus the Pb-O hybridization is strongest in the titanate and the transition-metal–O hybridization is strongest in the zirconate.

Zhong, King-Smith, and Vanderbilt[20] have calculated Born effective charges, Z^*, for eight perovskite ferroelectric and related materials, with B site cations Ti, Zr, and Nb. These results, as well as calculations for $KNbO_3$,[21,23] show very large values of Z^* for the B site cations and for O motions along the B-site cation to O bond. Z^* for this O component, $Z_1^*(\mathrm{O})$, ranges from -4.74 in $BaZrO_3$ to -7.01 in $KNbO_3$ and $NaNbO_3$. For cubic perovskite structure $PbZrO_3$, they find $Z_1^*(0)=-4.81$, while $Z^*(\mathrm{Zr})=5.85$. As emphasized by these authors, such high values are due to transition-metal–O covalency, and reflect the importance of this covalency to the lattice dynamics and particularly to the ferroelectric behavior. $PbTiO_3$ and $PbZrO_3$ also show values of $Z^*(\mathrm{Pb})$ higher by approximately 1 relative to the corresponding Ba compounds. This no doubt is related to the hybridization involving Pb orbitals as discussed above.

Harmonic lattice vibrations about the cubic perovskite structure are almost certainly not relevant to the physical properties of $PbZrO_3$, which has large atomic displacements from this structure. Nonetheless, they are of use in understanding differences in bonding from related materials and the instabilities leading to the observed structure. The transverse optic (TO) modes at the zone center were calculated for the equilibrium lattice parameter of 4.12 Å using a frozen-phonon approach, Two symmetries are allowed. These yield three infrared-active Γ_{15} modes, not counting the zero-frequency acoustic modes, and a Raman-active Γ_{25} mode.

For the Γ_{25} mode, which involves only O displacements, the total energy was calculated as a function of the mode amplitude. The calculation was performed within a tetragonal symmetry cell with one O and the cations fixed, and the remaining two O ions displaced in opposite directions along the tetragonal axis. The energy was then fitted to an even order polynomial and the quadratic term extracted to compute the phonon frequency. This yields a harmonic frequency of 40 cm^{-1}. However, this mode is very strongly anharmonic, with a large positive quartic term. In contrast, calculations for $KNbO_3$ yield a relatively stiff harmonic Γ_{25} mode at 266 cm^{-1}. The Γ_{25} displacement pattern involves only shearing of Zr-O bonds, but both shearing and stretching of Pb-O bonds; the soft anharmonic character of this mode, and the rapid stiffening for large displacements reflect the rather large Pb-O distance of 2.91 Å in the cubic perovskite structure.

For the Γ_{15} modes, forces were calculated for several small displacement patterns within a rhombohedral symmetry cell. These were used to fit the components of the reduced dynamical matrix, from which the frequencies and eigenvectors were obtained. The resulting Γ_{15} TO "phonons" are an unstable ferroelectric mode at $140i$ cm^{-1} and stable modes at 160 and 580 cm^{-1}.

RHOMBOHEDRAL FERROELECTRIC AND R-POINT INSTABILITIES

In order to better quantify the ferroelectric instability, the lowest energy atomic configuration was determined within a rhombohedral symmetry ($R3m$) cell consistent with the observed rhombohedral ferroelectric structure with small Ti doping. Rhombohedral strains were neglected since they are extremely small ($\sim 0.1°$) in this material.[10] The lowest energy configuration was determined initially by following the eigenvector of the unstable Γ_{15} mode and then by relaxing the structure through minimization of the atomic forces.

The atomic positions in the reference cubic perovskite structure were taken as (0,0,0) for Zr, (0.5,0.5,0.5) for Pb and (0.5,0,0),(0,0.5,0), and (0,0,0.5) for the three O ions, all in units of the lattice parameter (4.12 Å). The Pb ion was used as a fixed reference point, with respect to which the Zr ion was displaced to $(\delta_{\mathrm{Zr}},\delta_{\mathrm{Zr}},\delta_{\mathrm{Zr}})$ and the O to $(0.5+\delta_{\mathrm{o1}},\delta_{\mathrm{o2}},\delta_{\mathrm{o2}})$ and permutations. In these coordinates, the minimum energy configuration was found to be $\delta_{\mathrm{Zr}}=0.0448$, $\delta_{\mathrm{o1}}=0.0605$, and $\delta_{\mathrm{o2}}=0.0904$. This results in Pb-O bond-length changes of 0.53 Å, and smaller Zr-O bond-length changes of 0.27 Å. These are accompanied by an energy lowering of 0.253 eV. For comparison, $KNbO_3$, which actually has a rhombohedral ferroelectric ground state, has O displacements more nearly along the [111] axis, yielding Nb-O bond-length changes of 0.22 Å and changes in K-O distances of less than 0.1 Å; the energy gain for $KNbO_3$ is only 0.03 eV.[15] Thus the main differences from $KNbO_3$ (and $BaTiO_3$) are the much larger A site cation-O

bond-length changes, and the nearly order of magnitude larger instability energy.

This very large energy imposes an important constraint. Since the actual ground state is antiferroelectric, the instability leading to it must be even stronger. However, quite low levels of Zr substitution by isoelectric Ti yield a Rhombohedral ferroelectric ground state, and this state also can be induced at elevated temperatures. Thus the AFO structure must still be close in energy to the ferroelectric structure. Structures that may be derived from an R point antiferroelectric instability alone (doubled unit cell) apparently do not occur. On the other hand, Zhong and Vanderbilt,[22] based on LDA phonon calculations for a number of perovskites, and other considerations, attribute the antiferroelectric ground state of $PbZrO_3$ to a strong R-point antiferrodistortive instability, which overcomes the ferroelectric instability. Within this picture, the actual complex ground-state structure arises from additional distortions presumably contributing relatively little additional energy. This is consistent with the trends that they find, as well as detailed calculations that show no R point instabilities for ferroelectric $KNbO_3$.[14,23]

Structural minimizations were performed, again using force calculations, with a doubled rhombohedral unit cell, consistent with an R-point instability. The calculation allowed alternating Pb displacements along [111] and distortions of the oxygen octahedra consistent with this symmetry. Additionally a doubled tetragonal symmetry cell allowing alternating rotations of the O octahedra was relaxed. In both cases instabilities are found, consistent with the results of Zhong and Vanderbilt.[22] The minimized structure for the rhombohedral cell consisted of approximately 3° rotations of the O positions (with distortions of the O octahedra) and alternating 0.26 Å displacements of the Pb ions. However, the energy gain is only 0.06 eV per formula unit relative to the undistorted structure, as compared to 0.253 eV for the ferroelectric distortion. The tetragonal cell yielded a larger instability, corresponding to 12° rotations of the O octahedra with an energy gain of 0.200 eV per formula unit. The weaker instabilities at R relative to Γ and the actual ground-state AFO structure (see below), are consistent with the fact that pure R derived structures are not observed in $PbZrO_3$ as a function of temperature or weak doping. Both of the R-point instabilities result in large changes in Pb-O distances, but not Zr-O distances. This is qualitatively similar to the Γ point instability and again illustrates the importance of Pb-O interactions in the PZT system. These, like the transition-metal–O interactions, have significant covalent character.

ANTIFERROELECTRIC STRUCTURE

The ground-state antiferroelectric structure of $PbZrO_3$ has been studied using x-ray and neutron diffraction by several workers. The first complete structure determination, by Jona *et al.*,[6] was based on a combination of x-ray diffraction, which reliably determined the lattice parameters and cation positions, and neutron diffraction for the O positions. Based on this data, they assigned an orthorhombic Pba2 space group and gave O positions. This space group is not, however, centrosymmetric and therefore would allow a ferroelectric polarization. Although, there have been at least two reports of very weak ferroelectricity in $PbZrO_3$,[24,25] other investigations have failed to detect any remanent polarization in $PbZrO_3$[26,27]

TABLE I. Calculated and experimental O positions of antiferroelectric $PbZrO_3$ within Pbam symmetry. F denotes the initial structure of Fujishita and Hoshino (Ref. 9); M denotes their structure based on a soft mode decomposition. The notation is as in Ref. 9.

Coordinate	Present	F	M
O1(x)	0.280	0.266	0.281
O1(y)	0.158	0.157	0.1537
O1′(x)	0.297	0.291	0.281
O1′(y)	0.096	0.093	0.0963
O2(x)	0.030	0.029	0.035
O2(y)	0.261	0.259	0.259
O2(z)	0.282	0.280	0.2791
O3(z)	0.206	0.207	0.2209
O4(z)	0.226	0.252	0.2209

More recently, Fujishita and Hoshino,[7,9] also using neutron diffraction, assigned the centrosymmetric Pbam space group, and refined two separate sets of oxygen coordinates. The later of these[9] was based on a sum of simpler unstable R and X point modes in the perovskite structure.

Total-energy calculations were performed for the structure of Jona *et al.* and the two structures of Fujishita and co-workers. These were done directly using 40 atom supercells. The structure of Pba2 structure of Jona *et al.* yielded a total energy even less favorable than the cubic perovskite structure, presumably because of experimental uncertainty in the O positions. The two structures of Fujishita and co-workers yielded the same energy to within the precision of the present calculations. This energy is 0.233 eV per formula unit below the cubic perovskite structure but still 0.02 eV above the rhombohedral ferroelectric structure determined above.

This would seem to imply stability of the ferroelectric structure and no antiferroelectric ground state. However, the calculations reveal substantial forces on the O atoms in both of these structures. Accordingly, calculations were undertaken to relax the O positions within a Pbam cell. Since the experimental lattice parameters and cation positions have much smaller experimental uncertainties they were held fixed. The nine independent O coordinates obtained in this way are reported in Table I, along with values of Fujishita and co-workers. The differences between the calculated and experimental coordinates are of the same size as differences between the two experimental determinations. However, the differences, which include shifts exceeding 0.2 Å, are above the usual errors in LDA calculations suggesting that the calculated structure may be more reliable. A detailed neutron refinement would be very valuable in sorting out these discrepancies.

The calcaluted energy, with the relaxed O positions, is 0.274 eV below the cubic perovskite structure, and 0.021 eV (250 K) below the ferroelectric structure on a per formula unit basis. This is in accord with an antifereroelectric ground state as observed. Although cation forces with this structure are not very large (0.4 eV/Å for the Pb(1) ion, 0.1 eV/Å for Pb(2) and 0.3 eV/Å for Zr) it may be expected that cation relaxations would yield a small additional energy lowering.

SUMMARY AND CONCLUSIONS

$PbZrO_3$ has been studied using LDA electronic structure and total-energy calculations. The electronic structure displays both Pb-O and Zr-O hybridization. The Pb-O hybridization is weaker than in $PbTiO_3$, and conversely the Zr-O covalency is stronger. The cubic perovskite structure is unstable against several distortions. A very substantial 0.253 eV instability towards a rhombohedral ferroelectric structure is found. However, after relaxation of the O coordinates, an antiferroelectric structure is slightly lower in energy than the ferroelectric structure, consistent with the observed ground state. The small energy difference between the ferroelectric and antiferroelectric structures is also consistent with the temperature and composition-dependent transition to a rhombohedral ferroelectric structure in PZT. The AFO ground-state structure of $PbZrO_3$ is due to a very delicate balance between competing instabilities, which differ in energy by only 10%. The ability of LDA calculations to distinguish the correct ground state is very encouraging, especially in view of the small energy differences involved. This, combined with the successful description of the ferroelectric $PbTiO_3$ system by Cohen and co-workers,[2,3] bodes well for LDA studies of the technologically important PZT alloy system.

ACKNOWLEDGMENTS

The author is thankful for numerous helpful discussions with L. L. Boyer, R. Yu, and H. Krakauer. This work was supported by the Office of Naval Research. Computations were performed using computers at the DoD high performance computing facility at NAVO and the Arctic Region Supercomputing Center.

[1] B. Jaffe, W. J. Cook, and J. Jaffe, *Piezoelectric Ceramics* (Academic, London, 1971).
[2] R. E. Cohen and H. Krakauer, Ferroelectrics **136**, 65 (1992).
[3] R. E. Cohen, Nature (London) **358**, 136 (1992).
[4] R. E. Cohen and H. Krakauer, Phys. Rev. B **42**, 6416 (1990).
[5] G. Shirane, Phys. Rev. **86**, 219 (1952).
[6] F. Jona, G. Shirane, F. Mazzi, and R. Pepinsky, Phys. Rev. **105**, 849 (1957).
[7] H. Fujishita, Y. Shiozaki, N. Achiwa, and E. Sawaguchi, J. Phys. Soc. Jpn. **51**, 3583 (1982).
[8] M. Tanaka, R. Saito, and K. Tsuzuki, J. Phys. Soc. Jpn. **51**, 2635 (1982).
[9] H. Fujishita and S. Hoshino, J. Phys. Soc. Jpn. **53**, 226 (1984).
[10] R. W. Whatmore and A. M. Glazer, J. Phys. C **12**, 1505 (1979).
[11] D. Singh, Phys. Rev. B **43**, 6388 (1991).
[12] O. K. Anderson, Phys. Rev. B **12**, 3060 (1975).
[13] S. H. Wei and H. Krakauer, Phys. Rev. Lett. **55**, 1200 (1985); D. J. Singh, *Planewaves, Pseudopotentials and the LAPW Method* (Kluwer Academic, Boston, 1994).
[14] D. J. Singh and L. L. Boyer, Ferroelectrics **136**, 95 (1992).
[15] D. J. Singh, Ferroelectrics **164**, 143 (1995).
[16] L. Hedin and B. I. Lundqvist, J. Phys. C **4**, 2064 (1971).
[17] LAPW sphere radii of 2.30, 2.05, and 1.55 a.u. were used for Pb, Zr, and O, respectively. Local orbitals were used to include Pb $5d$, Zr $4s$, and $4p$, and O $2s$ states with the valence bands as well as to relax the linearization of the Zr $4d$ states.
[18] R. Yu, D. Singh, and H. Krakauer, Phys. Rev. B **43**, 6411 (1991).
[19] R. D. King-Smith and D. Vanderbilt, Phys. Rev. B **49**, 5828 (1994).
[20] W. Zhong, R. D. King-Smith, and D. Vanderbilt, Phys. Rev. Lett. **72**, 3618 (1994).
[21] R. Resta, M. Posternak, and A. Baldereschi, Phys. Rev. Lett. **70**, 1010 (1993).
[22] W. Zhong and D. Vanderbilt, Phys. Rev. Lett. **74**, 2587 (1995).
[23] R. Yu, C. Z. Wang, and H. Krakauer, Ferroelectrics **164**, 161 (1995); R. Yu and H. Krakauer, Phys. Rev. Lett. **74**, 4067 (1995).
[24] S. Robert, Phys. Rev. **83**, 1078 (1951).
[25] X. Dai, J. F. Li, and D. Viehland, Phys. Rev. B **51**, 2651 (1995).
[26] B. A. Scott and G. Burns, J. Am. Ceram. Soc. **55**, 331 (1972).
[27] O. E. Fesenko and V. G. Smortrakov, Ferroelectrics **12**, 211 (1976).